Flame Structure and Flame Spread Rate over a Solid Fuel in Partially Premixed Atmospheres

by

Kazuhiro YAMAMOTO, Yoshinori OGATA, Hiroshi YAMASHITA
Department of Mechanical Science and Engineering
Nagoya University, Furo-cho, Chikusa-ku, Nagoya, Aichi 464-8603, JAPAN

ABSTRACT

We have investigated the downward flame spread over a thin solid fuel. Hydrogen, methane, or propane, included in the gaseous product of pyrolysis reaction, is added in the ambient air. The fuel concentration is kept below the lean flammability limit to observe the partially premixing effect. Both experimental and numerical studies have been conducted. Results show that, in partially premixed atmospheres, both blue flame and luminous flame regions are enlarged, and the flame spread rate is increased. Based on the flame index, a so-called triple flame is observed. The heat release rate ahead of the original diffusion flame is increased by adding the fuel, and its profile is moved upstream. Here, we focus on the heat input by adding the fuel in the opposed air, which could be a direct factor to intensify the combustion reaction. The dependence of the flame spread rate on the heat input is almost the same for methane and propane/air mixtures, but larger effect is observed for hydrogen/air mixture. Since the deficient reactant in lean mixture is fuel, the larger effect of hydrogen could be explained based on the Lewis number consideration. That is, the combustion is surely intensified for all cases, but this effect is larger for lean hydrogen/air mixture ($Le < 1$), because more fuel diffuses toward the lean premixed flame ahead of the original diffusion flame. Resultantly, the pyrolysis reaction is promoted to support the higher flame spread rate.

Introduction

Generally, fire disaster is a phenomenon in which flames ignite various inflammables, such as liquid and solid fuels, which expands the combustion region. Therefore, in order to mitigate the losses in fire, it is essential to understand the flame spread mechanism [1-8]. However, in the actual fire, a number of factors, such as the ambient atmosphere, the flow field, and the shape and material of an inflammable solid, become entangled with each other. The phenomena of flame spread are therefore complex process. So far, many studies on the flame spread over inflammable solids have been performed, often using samples such as filter papers and polymethyl methacrylate (PMMA) materials to simulate the flame spread in fire [9-14].

In these studies, most of researches are dealing with ambient effect of dilution or reduction of oxygen concentration, which provide us useful information for the fire extinguishers to construct better fire suppression strategies. However, in the real case, the complete burning does not always occur, and some flammable products could remain. Under poorly ventilated conditions, the combustible mixtures of oxygen and fuel vapors may be formed, so that oxygen is partially depleted from the air and is replaced by combustible gases such as fuel vapors [15]. Subsequent fire spread over the solid fuel could occur in partially premixed atmospheres. In that case, it seems unclear whether the partially premixing effect is treated as encouraging the extinction (lower Damköhler number, Da) or intensifying the combustion reaction (higher Da).

Ronney et al., [15] have investigated the flame spread over the thin solid fuel in partially premixed atmospheres. In their asymptotic analysis, it is assumed that the combustion field consists of two regions, the non-premixed flame of solid fuel and premixed flame of added gaseous fuel. Their approach is within the framework of de Ris's model assuming the infinite reaction rate for non-premixed flame. If the oxygen concentration may be much higher than that of air, this assumption would be valid with high Da. However, since the vitiated conditions in fire imply oxygen concentrations below that of air, their approach may not be

valid. Therefore, the further study is needed for the experiments, coupled with numerical simulation with finite chemistry.

In the present study, we use a cellulose filter paper as a solid fuel. In experiments, we investigate the flame spread over a filter paper. To evaluate the partially premixing effect, different fuels of hydrogen, methane, and propane included in pyrolysis products [16,17] are added in the ambient air. The fuel concentration is kept below the lean flammability limit. Additionally, we conduct numerical simulation of downward flame spread for discussing the flame structure in detail.

Experimental setup

To control the conditions of ambient atmospheres, we used a wind tunnel system. The experimental setup is shown in **Fig. 1** (unit: mm). Opposed flow of fuel and air was supplied, and the filter paper was placed at the wind tunnel exit. In this experiment, the velocity of opposed flow, U_{in}, was kept at 25 cm/s. The cross section of the wind tunnel exit is 80 mm × 80 mm. Hydrogen, methane, or propane was added in the air to form a partially premixed mixture. The fuel concentration was kept below the lean flammability limit. The values for hydrogen, methane, and propane are 4.0, 5.0, and 2.1 % in volume.

Fig.1

A thin filter paper was used in this experiment. Two types of filter were used (produced by Toyo filter company). The properties of thickness, δ, and density, ρ, are 0.12 mm and 800 mg/cm^3 for sample No.1 and 0.25 mm and 560 mg/cm^3 for sample No.2. The filter width is 40 mm. The filter was ignited by a Nichrome wire for the two-dimensional flame spread. To void the effect of ignition, the flame spread rate was measured 20mm below the ignition point. In our preliminary experiment [10], it has been confirmed that the downward flame spread rate (V_f) of these two samples, coupled with other three filters of different thickness and density, is proportional to $1/(\rho\delta)$, which means that the value of $\rho\delta V_f$ is constant, corresponding to so called "thermally

thin" region [1].

Numerical method

To discuss the flame spread in partially premixed atmospheres in detail, numerical simulation was conducted. **Figure 2** shows the analytical model for downward flame spread over the solid fuel. The flame spread is considered in two-dimensional coordinate system. The governing equations in gas phase and solid phase are explained, separately.

Fig.2

Gas phase

The following equations are considered, maintaining conservation of mass, momentum, energy, and species *i* for compressible flow [18-22].

Continuity Equation

$$\frac{\partial \rho}{\partial t}+\frac{\partial(\rho u)}{\partial x}+\frac{\partial(\rho v)}{\partial y}=0 \qquad (1)$$

Momentum Equation

$$\frac{\partial(\rho u)}{\partial t}+\frac{\partial(\rho u^2)}{\partial x}+\frac{\partial(\rho uv)}{\partial y}=-\frac{\partial p}{\partial x}+\frac{\partial}{\partial x}\left(\mu\frac{\partial u}{\partial x}\right)+\frac{\partial}{\partial y}\left(\mu\frac{\partial u}{\partial y}\right)-\rho g \qquad (2)$$

$$\frac{\partial(\rho v)}{\partial t}+\frac{\partial(\rho v^2)}{\partial y}+\frac{\partial(\rho uv)}{\partial x}=-\frac{\partial p}{\partial y}+\frac{\partial}{\partial x}\left(\mu\frac{\partial v}{\partial x}\right)+\frac{\partial}{\partial y}\left(\mu\frac{\partial v}{\partial y}\right) \qquad (3)$$

Energy Equation

$$c_p\left[\frac{\partial(\rho T)}{\partial t}+\frac{\partial(\rho uT)}{\partial x}+\frac{\partial(\rho vT)}{\partial y}\right]=\frac{\partial}{\partial x}\left(\lambda\frac{\partial T}{\partial x}\right)+\frac{\partial}{\partial y}\left(\lambda\frac{\partial T}{\partial y}\right)-\sum_i h_i w_i \qquad (4)$$

Species Equation

$$\frac{\partial(\rho Y_i)}{\partial t}+\frac{\partial(\rho u Y_i)}{\partial x}+\frac{\partial(\rho v Y_i)}{\partial y}=\frac{\partial}{\partial x}\left(\rho D_i \frac{\partial Y_i}{\partial x}\right)+\frac{\partial}{\partial y}\left(\rho D_i \frac{\partial Y_i}{\partial y}\right)+w_i \qquad (5)$$

Ideal-Gas Equation

$$p=\rho R^0 T\sum_i \frac{Y_i}{m_i} \qquad (6)$$

The approach is to solve a set of time-dependent, coupled partial differential equations with a finite volume method by Patankar's SIMPLE method [23]. It should be noted that the steady-state flame spread is not assumed. In the simulation, only methane is added in the ambient air. Also, methane is the sole gaseous fuel formed in the pyrolysis reaction. The over-all one step reaction is adopted as $CH_4 + 2O_2 \rightarrow CO_2 + 2H_2O$. The reaction rate is expressed by

$$\omega_{ov}=k_{ov}C_{CH4}^{a}C_{O2}^{b}\exp(-E/RT) \qquad (7)$$

where C_i is molar concentration. The reaction coefficient, k_{ov}, and the effective activation energy, E, are referred to Ref. [24]. The constants of a and b are 0.2 and 1.3, respectively [24]. For the simulation of downward flame spread, the gravity is included in Eq. (2). The thermodynamic properties for the species are obtained from the CHEMKIN database [25]. The transport properties are calculated according to a Smooke's simplified transport model [26].

Solid phase

In this simulation, the thermally thin model is adopted, where the solid fuel is regarded as being thin enough

to have an essentially uniform temperature distribution across its thickness [1]. The properties of solid fuel thickness and density are set to be those of sample No. 1. Then, the governing equations are as follows:

Mass Conservation Equation

$$\frac{\partial \rho_s}{\partial t} = -(1-\nu_c)K_s \qquad (8)$$

Mass Conservation Equation for Fuel

$$\frac{\partial(\rho_s Y_F)}{\partial t} = -K_s \qquad (9)$$

Energy Equation

$$\rho_s c_{ps} \tau \frac{\partial T_s}{\partial t} = \tau \Delta H_p K_s + \lambda_g \frac{\partial T_g}{\partial y} - \varepsilon\sigma\left(T_s^4 - T_{g,\infty}^4\right) \qquad (10)$$

where half thickness of solid fuel is τ = 0.06 mm (= δ/2), specific heat is c_{ps} =1.3 J/(g･K), heat of formation is ΔH_p =64 J/g, emissivity is ε =0.6 [27], and Stefan-Boltzmann constant is σ =5.67×10^{-8} W/(m^2･K^4). The reaction of solid phase is

[Fuel-Solid] → ν_c[Char] + ν_{cg}[Fuel-Gas] + (1-ν_c - ν_{cg}) [Inert-Gas] (11)

where ν_c = 0.14, and ν_{cg} = 0.23 in this calculation [27]. The pyrolysis reaction rate is

$$K_s = A_s \rho_{s0} \left(\frac{\rho_s Y_F}{\rho_{s0}}\right)^c \exp\left(-\frac{E_s}{R^0 T_s}\right) \qquad (12)$$

where A_s =5.0 × 10^{16}1/s, c = 1.2, E_s =237 kJ/mol [27], and initial density of solid fuel is ρ_{s0}=800 mg/cm^3.

The computational domain in **Fig. 2b** is 90 mm (x) × 20 (y) mm, where x is the (opposite) direction of the flame spread and y is the direction perpendicular to the solid fuel surface. The grid size is 0.1 mm. In experiments, the filter sample was placed at the wind tunnel exit, which is set at x = 0 mm in the simulation. The heat source of 1500 K is added to ignite the filter. Its location is at 57.5 mm < x < 62.5 mm. In converge study, we changed the grid size, and confirmed that the simulated flame spread rate does not depend on the grid size. Boundary conditions are as follows:

(1) Inlet (x = 0 mm)

$$u = U_{in} = 0.25 \text{ m/s}, \quad v = 0, \quad T = 300 \text{ K}, \quad Y_i = Y_{i,in} \qquad (13)$$

(2) Exit (x = 90 mm)

$$\frac{\partial u}{\partial x} = 0, \quad \frac{\partial v}{\partial x} = 0, \quad \frac{\partial T}{\partial x} = 0, \quad \frac{\partial Y_{\mathrm{CH4}}}{\partial x} = \frac{\partial Y_{\mathrm{O2}}}{\partial x} = \frac{\partial Y_{\mathrm{CO2}}}{\partial x} = \frac{\partial Y_{\mathrm{H2O}}}{\partial x} = 0 \qquad (14)$$

(3) Upper boundary (y = 20 mm)

$$\frac{\partial u}{\partial y} = 0, \quad \frac{\partial v}{\partial y} = 0, \quad \frac{\partial T}{\partial y} = 0, \quad \frac{\partial Y_{\mathrm{CH4}}}{\partial y} = \frac{\partial Y_{\mathrm{O2}}}{\partial y} = \frac{\partial Y_{\mathrm{CO2}}}{\partial y} = \frac{\partial Y_{\mathrm{H2O}}}{\partial y} = 0 \qquad (15)$$

(4) Lower boundary between solid phase and gas phase (y = 0 mm)

$$u = 0, \quad v = v_f = \frac{\dot{m}}{\rho_g}, \quad T_g = T_s, \quad \dot{m} Y_{\mathrm{CH4}} - \rho_g D_{\mathrm{CH4}} \frac{\partial Y_{\mathrm{CH4}}}{\partial y} = \nu_{cg} K_s \tau, \quad \dot{m} Y_{\mathrm{O2}} - \rho_g D_{\mathrm{O2}} \frac{\partial Y_{\mathrm{O2}}}{\partial y} = 0 \qquad (16)$$

Results

Experimental results

Figure 3 shows direct photographs of flames over a sample No. 2 in methane/air mixtures. The fuel concentration, C_f, is 0 and 2 % in volume. The front views of the flame are shown. As seen in this figure, the flame structure is almost two-dimensional. When the fuel is added in the opposed air, both blue flame and luminous flame regions are enlarged.

Fig.3

Figure 4 shows the measured flame spread rate, V_f, in hydrogen, methane, or propane/air mixtures. Since the fuel supply is kept below the flammability limit, the range of the fuel concentration is different. As seen in this figure, when the fuel is added, the flame spread rate is increased for all cases. Although the flame spread rate of sample No. 1 is higher than that of No. 2, the increasing rate is almost the same in hydrogen, methane, and propane/air mixtures. Hence, independent of the added fuel type, the partially premixing effects could be interpreted as increasing Da. To explain this effect, we simulated the flame spread.

Fig.4

Simulation results

Figure 5 shows the temperature profile at t = 2.0 s. Time is counted after the ignition. The fuel concentration in the opposed flow is 0 and 2 % in volume. It is found that high temperature region is slightly expanded and the maximum temperature is higher by 40 K in partially premixed atmospheres. Based on the flame position, the flame spread rate is calculated. The steady flame motion is achieved for 1.0 ~ 2.5 s. The obtained flame spread rate is 1.47, 1.67, 1.87 mm/s for C_f = 0, 1, 2%, respectively. Comparing the results in **Fig. 4**, the numerical model slightly underestimates the flame spread rate. This could be because the reaction scheme in numerical model is the over-all one step reaction. Also, the detailed pyrolysis gases are not considered. However, since its discrepancy with experiments is not large, it is possible to examine the flame spread in partially premixed atmospheres qualitatively.

Fig.5

Figure 6 shows the distributions of the surface temperature of the solid fuel, T_s, and the fuel ejection velocity, v_f, at $t = 2.5$ s for $C_f = 0$ and 2%. As shown in this figure, the high-temperature region of the solid surface is expanded as C_f is increased. Resultantly, the fuel ejection velocity is larger. Hence, as C_f is increased, more fuel is ejected into the gas phase. Therefore, an increase in the flame spread rate is apparently caused by the promotion of the pyrolysis reaction. In the following section, we investigate the flame structure in detail.

Fig.6

Discussion

In order to discuss the partially premixing effect, the flame structure is examined, by using the flame index, G_{FO}, which is a good parameter to distinguish the region of diffusion flame or the premixed flame [20].

$$G_{FO} = \mathrm{grad}(Y_f) \cdot \mathrm{grad}(Y_o) \qquad (\text{for } q/q_{\max} > 0.01) \quad (17)$$

where G_{FO} is positive for a premixed flame and negative for a diffusion flame, q is the heat release rate, and $q_{\max}$ is the maximum heat release rate. **Figure 7** shows the distributions of the heat release rate at $t = 2.5$ s for $C_f = 0\%$ and 2%. As seen in this figure, the region of large heat release rate is expanded around the flame tip. Interestingly, two reaction zones are recognized when the fuel is added in the ambient air. For comparison, the flame index at the same period is shown in **Fig. 8**. To discuss the flame structure in detail, the area around the leading flame tip is enlarged in **Fig. 9**. As shown in these figures, two premixed flames are formed near the diffusion flame (DF).

Fig.7

Fig.8

Fig.9

It should be noted that the premixed flame can be classified based on mixedness [20], by which the fuel-lean and fuel-rich regions are identified. It is found that, in **Fig. 9**, the premixed flame near the solid fuel surface is the rich premixed flame (RPF), and the premixed flame ahead of the diffusion flame is the lean premixed flame (LPF). Thus, a so-called triple flame is observed in the combustion field over the solid fuel. Clearly in **Fig. 9**, when the fuel is added in the opposed flow, the lean premixed flame is intensified whereas

the rich premixed flame is weakened.

To study further, one-dimensional distributions of mass fractions of methane and oxygen, heat release rate, flame index at $y = 2.5$ mm are investigated. These profiles obtained at $t = 2.5$ s are shown in **Fig. 10**. It is found that, in partially premixed atmospheres, the maximum heat release rate is not larger. Instead, the heat release rate in the region ahead of the original diffusion flame is increased by adding the fuel, and its profile is moved upstream. Resultantly, the pyrolysis reaction is promoted to support the higher flame spread rate. Since some part of oxygen is consumed in the lean premixed flame, the rich premixed flame near the solid fuel surface is weakened.

Fig.10

Therefore, the heat transfer caused by the added fuel is the key to discuss the flame spread in partially premixed atmospheres. It should be noted that even if the fuel concentration is the same, the heat of combustion is different among hydrogen, methane, and propane. Then, we calculate the heat input by adding the fuel, which could be a direct factor to intensify the reaction in the flame region.

$$Q_T = C_f V Q_f \qquad (18)$$

where V is the molar rate determined by the density and component of mixture, and Q_f is the molar heat of reaction. Results are shown in **Fig. 11**. To make clear the effect of fuel addition, the flame spread rate is non-dimensionalized by the one in the opposed air, $V_{f,0}$. The values of $V_{f,0}$ are 1.909 mm/s (No.1) and 1.221 mm/s (No.2) for CH_4, 1.898 mm/s (No.1) and 1.275 mm/s (No.2) for H_2, 1.870 mm/s (No.1) and 1.280 mm/s (No.2) for C_3H_8. It is interesting to note that, in case of methane and propane, the dependence on the heat input is almost the same. However, for the hydrogen, the larger effect is observed.

Fig.11

Since the deficient reactant is fuel in lean premixed mixture, it is important to consider the Lewis number (Le=K/D), where K is the thermal diffusivity and D is the diffusion coefficient [14,28]. It is well

known that, roughly Le = 1 for lean methane/air mixture, Le > 1 for lean propane/air mixture, and Le < 1 for lean hydrogen/air mixture. Therefore, the combustion in LPF could be largely promoted for lean hydrogen/air mixture, because more hydrogen diffuses toward the lean premixed flame to increase the heat release rate in the region ahead of the original diffusion flame. Then, the pyrolysis reaction is promoted, resulting in an increase of flame spread rate.

Conclusions

In this study, we have investigated the downward flame spread over the thin solid fuel experimentally and numerically. To consider poorly ventilated conditions in fire, hydrogen, methane, or propane is added in the ambient air. The fuel concentration is kept below the lean flammability limit to observe the partially premixing effect. The following conclusions are made.

(1) In the partially premixed atmospheres, both blue flame and luminous flame regions are enlarged, and the flame spread rate is increased. Although the flame spread rate of sample No. 1 is higher than that of No. 2, the increasing rate is almost the same in hydrogen, methane, and propane/air mixtures. Hence, independent of the added fuel type, the partially premixing effects could be interpreted as increasing Da.

(2) The flame structure is examined in terms of the flame index. The so-called triple flame is observed in the combustion field over the solid fuel. When the fuel is added in opposed flow, the heat release rate in the region ahead of the original diffusion flame is increased. Since some part of oxygen is consumed in the lean premixed flame, the rich premixed flame near the solid fuel surface is weakened.

(3) By calculating the heat input of added fuel in the opposed air, the dependence of flame spread rate on the heat input is almost the same for methane and propane/air mixtures, but larger effect is observed for

hydrogen/air mixture. Since more hydrogen diffuses toward the lean premixed flame, the pyrolysis reaction is promoted to support the higher flame spread rate.

Acknowledgments

The authors thank Prof. G. Kushida of Aichi Institute of Technology for very helpful discussions.

References

1. J. N. de Ris, *Proc. Combust. Inst.,* 12 (1969) 241-252.
2. T. Hirano, and K. Sato, *Proc. Combust. Inst.* 15 (1975) 233-241.
3. A. C. Fernandez-Pello, and T. Hirano, *Combust. Sci. and Tech.* 32 (1983) 1-31.
4. I. S. Wichman, *Prog. Energy Combust. Sci*. 18 (1992) 553-593.
5. C. Di Blasi, *Combust. Flame* 97 (1994) 225-239.
6. W. E. Mell, and T. Kashiwagi, *Proc. Combust. Inst.* 27 (1998) 2635-2641.
7. H. Y. Shih, and J. S. T'ien, *Proc. Combust. Inst.* 28 (2000) 2777-2784.
8. A. Umemura, et al., *Proc. Combust. Inst.* 29 (2002) 2535-2543.
9. M. Suzuki, R. Dobashi, and T. Hirano, *Proc. Combust. Inst.* 25 (1994) 1439-1446.
10. K. Yamamoto, K. Mori, and Y. Onuma, *Trans. Japan Society for Mechanical Engineers*, B68-672 (2002) 2437-2443.
11. S. Takahashi, M. Kondou, K. Wakai, and S. Bhattacharjee, *Proc. Combust. Inst.* 29 (2002) 2579-2586.
12. A. Ishihara, Y. Sakai, K. Konishi, E. Andoh, *Proc. Combust. Inst.* 30 (2005) 2123-2130.
13. K. Takahashi, A. Ito, Y. Kudo, T. Konishi, K. Saito, *Proc. Combust. Inst.* 30 (2005) 2271-2277.

14. K. Tolejko, I. I. Feier, J. S. T'ien, *Proc. Combust. Inst.* 30 (2005) 2263-2270.

15. P. D. Ronney, et al., *Combust. Flame* 100 (1995) 474-483.

16. C. F. Cullis, M. M. Hirschler, R. P. Townsend, and V. Visanuvimol, *Combust. Flame* 49 (1983) 249-254.

17. T. Kashiwagi, and H. Nambu, *Combust. Flame* 88 (1992) 345-368.

18. H. Yamashita, et al., *J. Heat Transfer* 115 (1993) 418-425.

19. K. Nakabe, et al., *Combust. Flame* 98 (1994) 361-374.

20. H. Yamashita, M. Shimada, and T. Takeno, *Proc. Combust. Inst.* 26 (1996) 27-34.

21. K. Yamamoto, S. Ishizuka, and T. Hirano, *Pro. Combust. Inst.* 26 (1996) 1129-1135.

22. Y. Nakamura, G. Kushida, H. Yamashita, T. Takeno, *Combust. Flame* 120 (2000) 34-48.

23. S. V. Patankar, *Numerical Heat Transfer and Fluid Flow*, McGraw-Hill, New York, 1980.

24. C. K. Westbrook, F. L. Dryer, *Combust. Sci. Technol*. 27 (1981) 31-43.

25. R. J. Kee, F. M. Rupley, and J. A. Miller, *Sandia National Laboratories Report* No. SAND89-8009 (1989).

26. M. D. Smooke, *Reduced Kinetic Mechanisms and Asymptotic Approximations for Methane-Air Flames*, Springer-Verlag, Berlin, Germany (1991).

27. T. Kashiwagi, et al., *Proc. Combust. Inst.* 26 (1996) 1345-1352.

28. K. Yamamoto, and S. Ishizuka, *JSME Int. J. Series B* 46(1) (2003) 198-205.

Figure captions

Fig. 1 Wind tunnel system for downward flame spread in partially premixed atmospheres.

Fig. 2 Analytical model for downward flame spread over solid fuel; (a) computational domain, and (b) boundary conditions.

Fig. 3 Direct photograph of flames over sample No. 2 in methane/air mixture; (a) C_f= 0%, (b) C_f= 2%.

Fig. 4 Measured flame spread rate using different fuels.

Fig. 5 Temperature profiles at t = 2.0 s are shown. Fuel is methane and filter is sample No. 1; (a) C_f= 0 %, (b) C_f= 2 %.

Fig. 6 Profiles of (a) surface temperature of the solid fuel, and (b) fuel ejection velocity; t = 2.5s. Fuel is methane and filter is sample No. 1.

Fig. 7 Contour maps of flame index at t = 2.5 s are shown. The added fuel is methane; (a) C_f= 0 %, (b) C_f= 2 %.

Fig. 8 Contour maps of heat release rate at t = 2.5 s are shown. The added fuel is methane; (a) C_f= 0 %, (b) C_f= 2 %.

Fig. 9 Contour maps of flame index at t = 2.5 s are shown. Area around the leading flame tip is enlarged. The added fuel is methane; (a) C_f= 0 %, (b) C_f= 2 %.

Fig. 10 Profiles of mass fractions of fuel and oxygen, heat release rate, and flame index at y = 2.5mm. These are obtained at t = 2.5 s. Added fuel is methane; (a) C_f= 0 %, (b) C_f= 2 %.

Fig. 11 Variations of flame spread rate with calculated heat input in partially premixed mixtures.

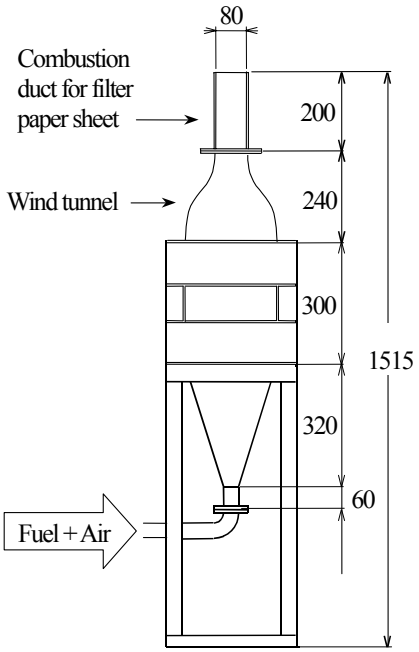

Fig. 1 Wind tunnel system for downward flame spread in partially premixed atmospheres.

[Word Count] = (85+10)*2.2*1 + 13 (caption) = 222 words

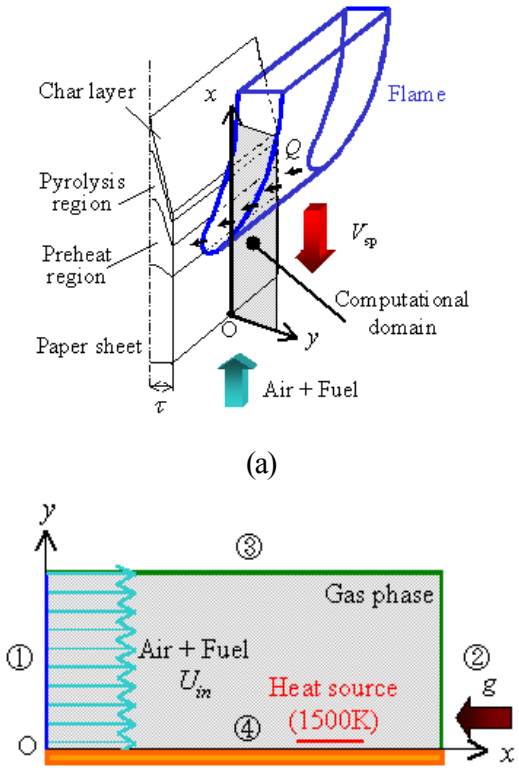

Fig. 2 Analytical model for downward flame spread over solid fuel; (a) computational domain, and (b) boundary conditions.

[Word Count] = (115+10)*2.2*1 + 18 (caption) = 293 words

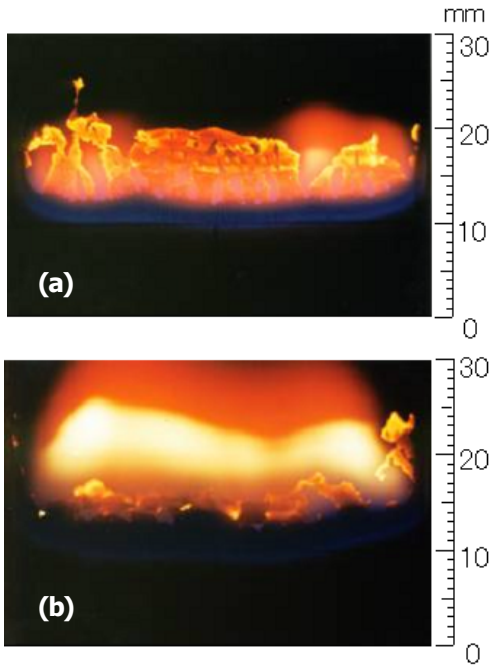

Fig. 3 Direct photograph of flames over sample No. 2 in methane/air mixture; (a) C_f = 0%, (b) C_f = 2%.

[Word Count] = (85+10)*2.2*1 + 22 (caption) = 231 words

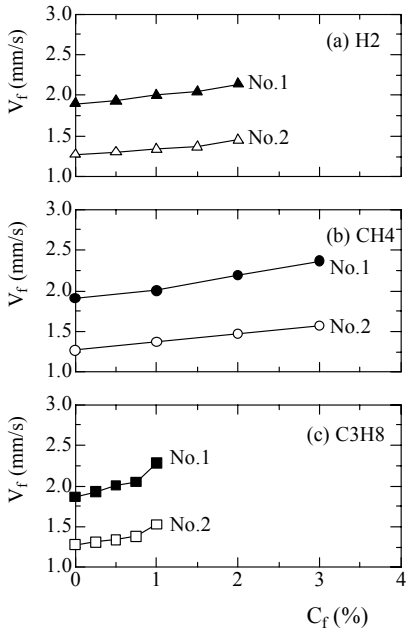

Fig. 4 Measured flame spread rate using different fuels.

[Word Count] = (80+10)*2.2*1 + 9 (caption) = 207 words

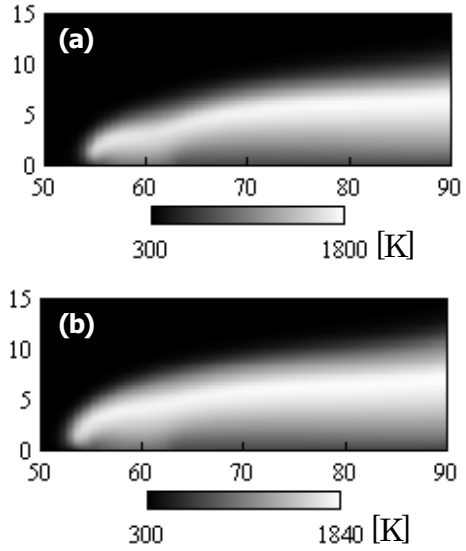

Fig. 5 Temperature profiles at $t = 2.0$ s are shown.
Fuel is methane and filter is sample No. 1; (a) $C_f = 0\%$,
(b) $C_f = 2\%$.

[Word Count] = (70+10)*2.2*1 + 24 (caption) = 200 words

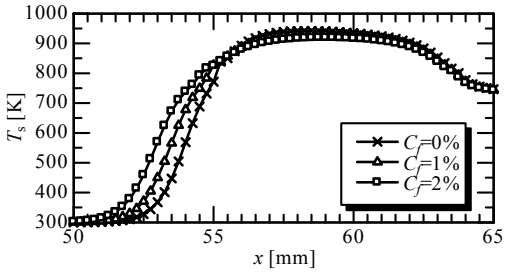

(a) Temperature

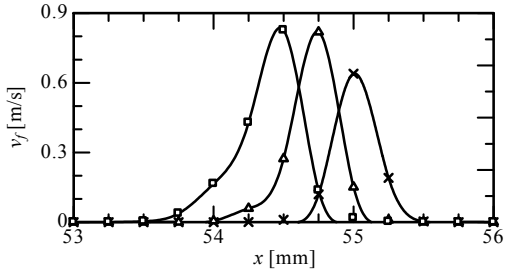

(b) Velocity of fuel ejection

Fig. 6 Profiles of (a) surface temperature of the solid fuel, and (b) fuel ejection velocity; t = 2.5s. Fuel is methane and filter is sample No. 1.

[Word Count] = (80+10)*2.2*1 + 16 (caption) = 214 words

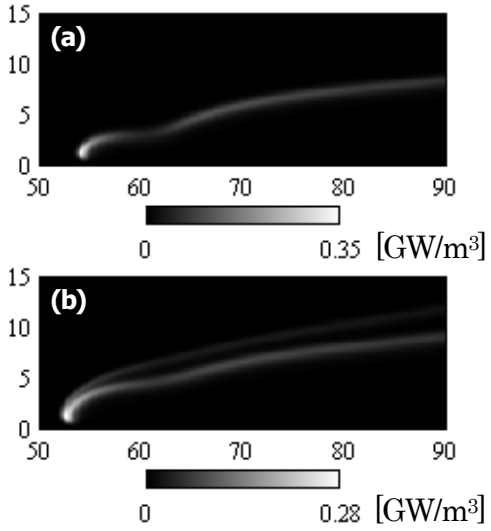

Fig. 7 Contour maps of heat release rate at $t = 2.5$ s are shown. The added fuel is methane; (a) $C_f = 0$ %, (b) $C_f = 2$ %.

[Word Count] = (70)*2.2*1 + 28 (caption) = 204 words

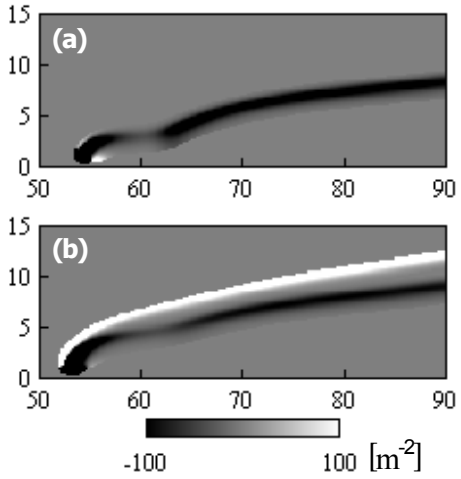

Fig. 8 Contour maps of flame index at $t = 2.5$ s are shown. The added fuel is methane; (a) $C_f = 0$ %, (b) $C_f = 2$ %.

[Word Count] = (65+10)*2.2*1 + 28 (caption) = 193 words

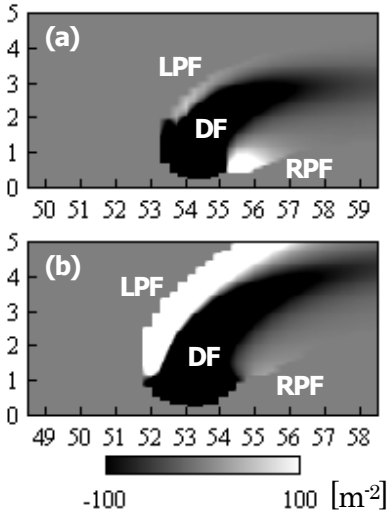

Fig. 9 Contour maps of flame index at $t = 2.5$ s are shown. Area around the leading flame tip is enlarged. The added fuel is methane; (a) $C_f = 0$ %, (b) $C_f = 2$ %.

[Word Count] = (65+10)*2.2*1 + 37 (caption) = 202 words

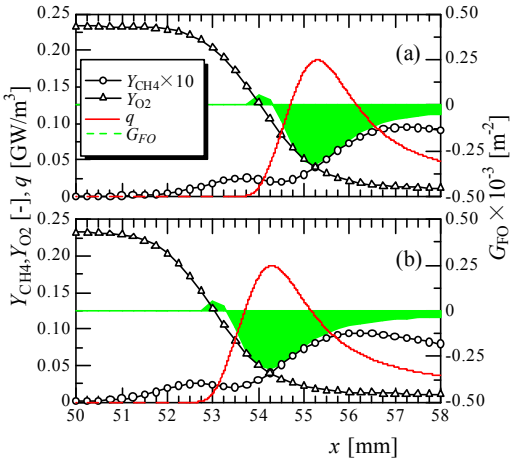

Fig. 10 Profiles of mass fractions of fuel and oxygen, heat release rate, and flame index at y = 2.5mm. These are obtained at t = 2.5 s. Added fuel is methane; (a) C_f = 0 %, (b) C_f = 2 %.
[Word Count] = (60+10)*2.2*1 + 42 (caption) = 196 words

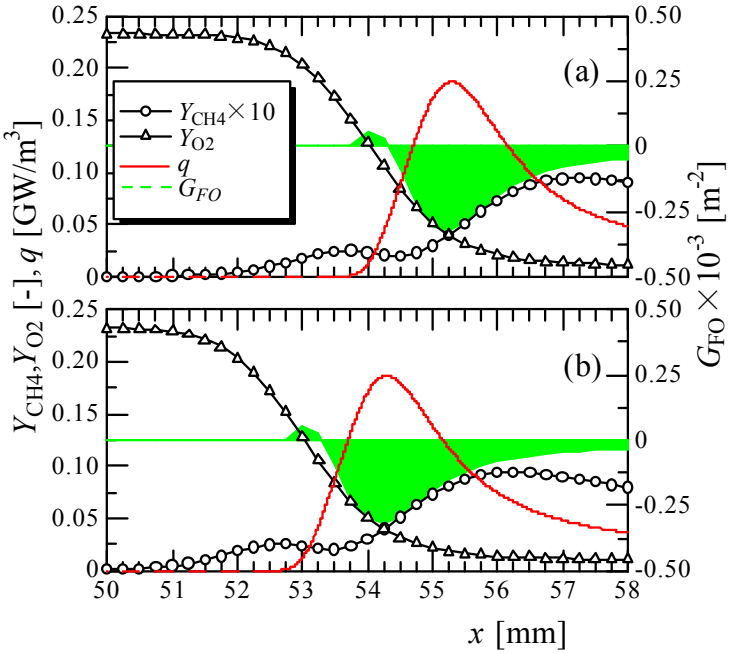

Fig. 10 (enlarged)

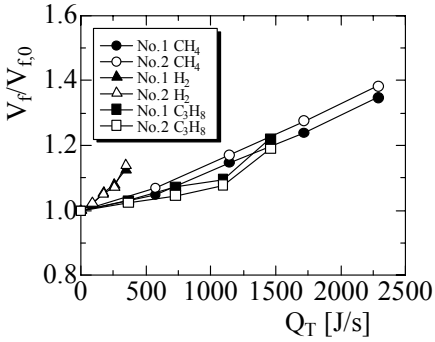

Fig. 11 Variations of flame spread rate with calculated heat input in partially premixed mixtures.

[Word Count] = (45+10)*2.2*1 + 15 (caption) = 136 words

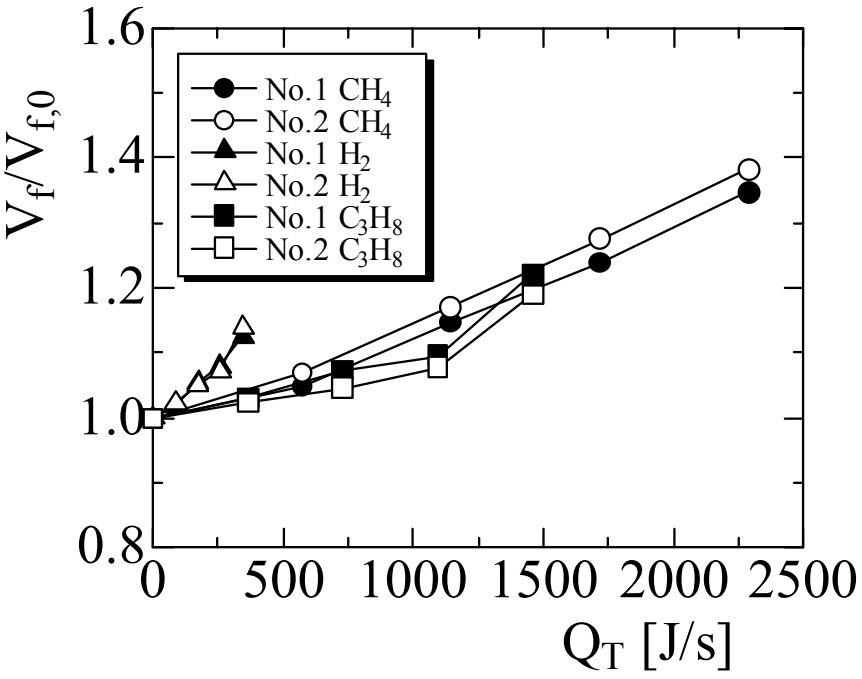

Fig. 11 (enlarged)